Impact of Antarctic mixed-phase clouds on climate

R. Paul Lawson[a,1] and Andrew Gettelman[b]

[a]SPEC Incorporated, Boulder, CO 80301; and [b]National Center for Atmospheric Research, Boulder, CO 80307

Edited by Mark H. Thiemens, University of California, San Diego, La Jolla, CA, and approved November 13, 2014 (received for review September 22, 2014)

Precious little is known about the composition of low-level clouds over the Antarctic Plateau and their effect on climate. In situ measurements at the South Pole using a unique tethered balloon system and ground-based lidar reveal a much higher than anticipated incidence of low-level, mixed-phase clouds (i.e., consisting of supercooled liquid water drops and ice crystals). The high incidence of mixed-phase clouds is currently poorly represented in global climate models (GCMs). As a result, the effects that mixed-phase clouds have on climate predictions are highly uncertain. We modify the National Center for Atmospheric Research (NCAR) Community Earth System Model (CESM) GCM to align with the new observations and evaluate the radiative effects on a continental scale. The net cloud radiative effects (CREs) over Antarctica are increased by +7.4 Wm^{-2}, and although this is a significant change, a much larger effect occurs when the modified model physics are extended beyond the Antarctic continent. The simulations show significant net CRE over the Southern Ocean storm tracks, where recent measurements also indicate substantial regions of supercooled liquid. These sensitivity tests confirm that Southern Ocean CREs are strongly sensitive to mixed-phase clouds colder than −20 °C.

Antarctica | climate | mixed-phase | clouds

Clouds have a major impact on the Earth's radiative budget and climate change (1, 2), yet a dearth of microphysical data have been collected within clouds over the Antarctic Plateau. This lack of microphysical data is associated with challenges deploying and operating instrumentation in the world's harshest, most remote atmospheric environment (3). Clouds have a critical influence on the Antarctic ice sheet's radiation budget and surface mass balance and appear to affect synoptic-scale effects over the Southern Ocean (3–6). Early (1986) airborne lidar measurements of cloud properties over the Antarctic Plateau indicated that the clouds consisted entirely of ice crystals (7). Because supercooled water drops are more likely to freeze as the temperature approaches the homogenous freezing point, about −37 °C in clouds (8), low-level Antarctic clouds, which are the coldest on Earth, have generally been treated as being all ice in numerical models. However, measurements reported in this article show that supercooled water drops can exist in low-level clouds at −32 °C.

Model sensitivity simulations demonstrate that uncertainties in the particle phase of Antarctic clouds can have a significant impact on the Antarctic continent, as well as even more far-reaching effects. In the late 1990s, the National Center for Atmospheric Research (NCAR) Community Climate Model version 2 was run with the standard 10-μm water drop clouds and compared with the output when the particles were changed to ice. The results showed that changing from water drops to 10-μm ice crystals produced 1°–2 °C temperature increases throughout the Antarctic troposphere (4). The microphysical properties of cloud particles can have a major impact on the Earth's radiation budget (6), and the cloud radiative forcing constitutes the major source of discrepancies between global climate models (GCMs) (9). Bias in the clouds over the Southern Ocean has been correlated with sensitivity to global climate (10).

This article focuses on the microphysical characteristics of clouds observed at the South Pole and their potential impact on Earth's radiation budget. In January–February 2009, a unique tethered balloon system (TBS) with a cloud particle imager (CPI) capable of high-resolution (2.3 μm pixel) digital images of cloud particles was operated at the South Pole (11). The CPI recorded digital images of particles passing through its viewing area during vertical profiles of low-level clouds. Simultaneous measurements were made with a vertically pointing micropulse lidar (MPL) (12). A strong correlation was found between in situ observations of mixed-phase clouds and MPL backscatter. In contrast, when all-ice clouds were observed, the MPL backscatter was significantly less because of the much smaller ensemble projected area of the ice particles. This strong differential signature motivated us to examine 365 d of continuous MPL measurements, compiling a dataset sorted into 10-min time segments of mixed-phase and all-ice cloud regions. The year-long South Pole results were extrapolated over the entire Antarctic Plateau and compared with simulations, using the NCAR Community Earth System Model (CESM) (13). The model results were analyzed to determine how the percentage of mixed-phase and all-ice clouds affected Earth's radiation budget.

Instrumentation

The instrument package on the TBS deployed at the South Pole included an aspirated CPI; a meteorological package with sensors for temperature, pressure, Global Positioning System position, wind direction, and speed; a cryogenic frost point hygrometer (14); and an ice nuclei filter system (15). CPI images are used to discriminate water drops from ice crystals. Examples of CPI images of water drops and ice crystals are shown in Fig. 1. The TBS was deployed up to altitudes of 700 m above the surface; the surface is about 2,840 m above mean sea level at the South Pole.

Measurements in Mixed-Phase and All-Ice Clouds

As shown in Fig. 1, CPI images clearly delineate water drops and ice particles in the low-level mixed-phase clouds observed over the South Pole at temperatures colder than −30 °C. The MPL lidar was operated continuously in a vertically pointing configuration during all TBS flights. Fig. 2*A* shows an example of level 1

Significance

Polar regions are foci of climate change, because of more-than-expected warming, problematic remote-sensing retrievals, and large uncertainties about cloud effects on radiation budgets. Antarctica is the world's most remote, coldest, and driest location. Until recently, researchers have assumed that low-level clouds over the frozen Antarctic Plateau consist mainly of ice crystals. Now, measurements with a unique tethered balloon system and a ground-based lidar show that nearly 50% of clouds in the austral summer contain supercooled water which has a significant impact on the radiative properties of Antarctic clouds. Modifying a global climate model to relax the freezing below −20 °C results in a strong simulated radiative (cooling) effect, affecting the entire Antarctic Continent and extending out into the Southern Ocean.

Author contributions: R.P.L. performed research; R.P.L. and A.G. analyzed data; and R.P.L. and A.G. wrote the paper.

The authors declare no conflict of interest.

This article is a PNAS Direct Submission.

Data deposition: The tethered balloon and lidar data, and the output from model runs have been deposited in the CISL Research Data Archive, ftp://ftp.cgd.ucar.edu/archive/andrew/lawson2015pnas/.

[1]To whom correspondence should be addressed. Email: plawson@specinc.com.

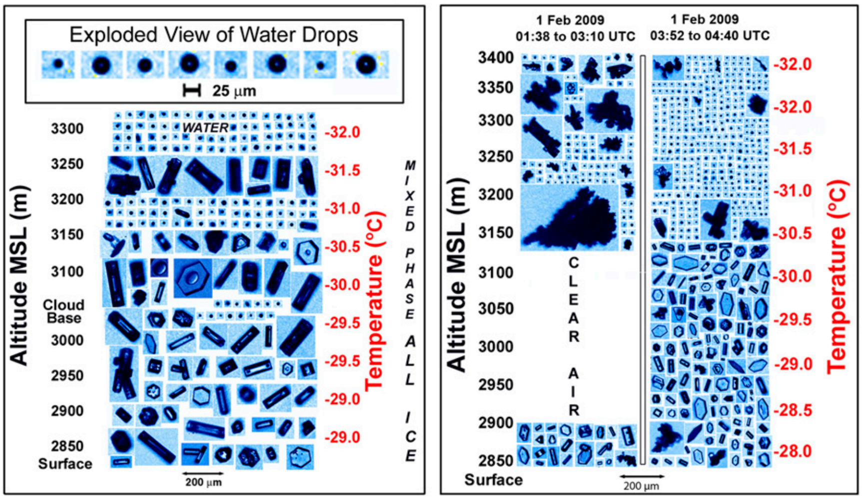

Fig. 1. Examples of CPI images shown as a function of altitude above mean sea level (MSL) in mixed-phase and all-ice clouds (*Left*) from 0214 to 0350 on 26 January 2009, and (*Right*) times shown on 1 February 2009.

backscatter from the MPL on 26 January 2009, when the TBS profiled down through the region of mixed-phase cloud and precipitating ice (Fig. 1). The measurements in Fig. 2*A* clearly show that MPL backscatter in the layer from about 3.2 to 3.5 km (−31.9 °C to −28.5 °C) is significantly greater than in the all-ice cloud that is precipitating in the region from about 3.15 km down to the surface. Note that the temperatures shown in Fig. 1 are from the TBS and temperatures in Fig. 2 are from the 00Z radiosonde. The backscatter ratio of water drops and ice crystals is directly proportional to the ensemble projected particle area, unless the ice crystals are horizontally oriented or multiple scattering is significant (16, 17). Multiple scattering is not a factor in the optically thin, low-level clouds sampled at close range over the South Pole. Backscatter enhancements from horizontally oriented ice crystals range from 0% to 6% in optically thick mixed-phase clouds and from 0% to 0.5% in cold ice clouds and are negligible for particles <100 μm. On the basis of the sizes and shapes of ice crystals observed in South Pole clouds and the concentration ratio of cloud drops to ice crystals (11, 18), we find that the backscatter contribution from horizontally oriented ice crystals is negligible in mixed-phase clouds over the South Pole.

The much higher backscatter ratio of mixed-phase to ice clouds is further validated in the scatter plot in Fig. 2*B*, which shows the level 1 MPL backscatter when the TBS was sampling all ice clouds (blue points) and when it sampled mixed-phase clouds (red points). The MPL backscatter measurements when the CPI was imaging ice crystals are clearly less intense than the backscatter intensity from mixed-phase clouds. In fact, there is a clear separation in ice and mixed-phase points at an MPL backscatter intensity level of 4.0. An MPL backscatter level >4.0 is therefore used to identify regions of mixed-phase clouds.

Fig. 2*C* shows a plot of the relative frequency of all-ice (blue points) and mixed-phase clouds (red points) that occurred for all of 2009, based on the criteria developed from Fig. 2*B*. In Fig. 2*C*, all of the 10-min average maximum MPL backscatter measurements in 2009 that correspond to a radiosonde temperature of <−37 °C (the temperature of homogeneous freezing of supercooled water observed in the atmosphere) (19) were used to identify all-ice clouds. It can be seen that only a few of the (blue) MPL backscatter points, all of which are at temperatures < −37 °C (all-ice), exceed the cutoff value of 4.0. The blue data points that exceed a lidar backscatter value >4.0 can generally be attributed to blowing snow, mostly during the austral winter. The red data points in Fig. 2*C* correspond with MPL values >4.0, with a corresponding radiosonde temperature ≥−37 °C. The red data points are classified as mixed-phase cloud, based on the correlation between MPL backscatter and CPI images shown in Fig. 2*B*.

The data in Fig. 2*C* are 10-min averages of continuous MPL coverage for all of 2009. These same data are plotted on a monthly basis in Fig. 2*D*. The most frequent occurrence of mixed-phase clouds is in the austral summer (December–February). In January and December, the frequency of all-ice and mixed-phase clouds was about equal. Mixed-phase clouds occurred throughout the entire austral winter in 2009, except in the month of August. The surface temperature inversion over the Antarctic Plateau in the winter can be very sharp. Even with surface temperatures 15 °C colder than the homogeneous freezing temperature of water, MPL lidar measurements suggest that elevated mixed-phase clouds can form in the dead of the austral winter.

The frequency of mixed-phase clouds is of interest from a clouds physics standpoint, because unlike the Arctic (20), the Antarctic clouds often occur at temperatures <−30 °C. The high frequency of occurrence of supercooled liquid water at these very cold temperatures is likely a result of the exceptionally clean air over the Antarctic Plateau. Although pure water can be supercooled to −40 °C in the laboratory, it is observed only rarely at temperatures <−30 °C in clouds. The most common observations are in wave clouds over mountain ranges (19, 21) and in deep, vigorous convection (22).

Climate models generally use ice nucleation schemes (23) based on empirical measurements typical of observations in the midlatitudes and tropics (21, 24). The models typically idealize the vapor deposition process as perfectly efficient (for deposition onto a pure ice surface in equilibrium). This implies that ice and liquid in clouds are well mixed down to the diffusion scale. Given subgrid variability in clouds, this is likely not the case in reality at the large (100 km) scale of global climate models. As a consequence of these assumptions, models generally freeze a large fraction of the available supercooled liquid at temperatures <−10 °C. According to the observations presented here, it may be necessary to modify the nucleation and freezing (vapor deposition) schemes in climate models that include the Antarctic Plateau. Because of their similar conditions, the frequent presence of mixed-phase clouds observed at the South Pole can be extrapolated over the entire Antarctic Plateau, which has an average elevation of about 3,000 m and covers about 785,000 square kilometers in the center of the continent. As suggested by climate model runs, clouds over Antarctica can have a strong influence on the earth's radiation budget and can even affect synoptic scale climate in the Southern Ocean and Tropics (3, 4). In the next section, we investigate the effect our observations of mixed-phase clouds may have on the radiation budget of Antarctica and the surrounding area.

Simulations with the NCAR GCM

To compare with the observations, experiments are performed with constrained versions of the atmospheric component of CESM, version 5.2 (23, 25). Perhaps most important for these

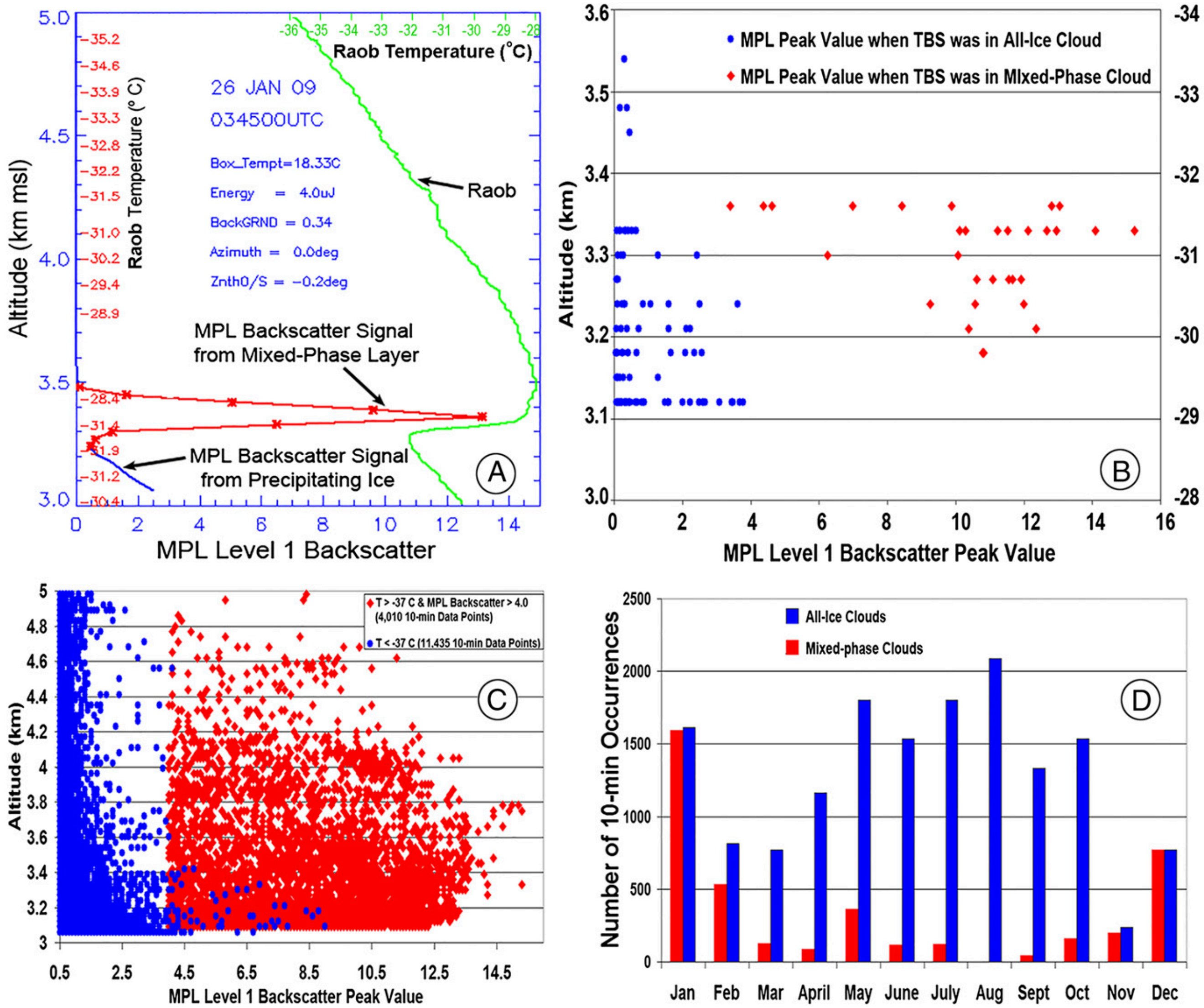

Fig. 2. (*A*) Plot of MPL level 1 10-min average (034000–035000 UTC) backscatter signal versus altitude on 26 January, 2009. The plot corresponds to the time when the TBS was descending through cloud from 3.4 km to the surface. The upper portion of cloud was mixed-phase, and the portion of cloud below about 3.2 km was precipitating ice (Fig. 1). The 00Z South Pole radiosonde observation (Raob) is plotted in green. Shown in blue text are MPL lidar housekeeping parameters. (*B*) Plot showing the maximum lidar backscatter as a function of the altitude when the TBS CPI was recording all-ice clouds (blue points) and mixed-phase clouds (red points). Temperature scale is representative of late January at the South Pole. (*C*) Scatter plot altitude versus MPL signal strength, where all-ice (blue points) and mixed-phase (red points) clouds are distinguished using the criteria shown in the legend. (*D*) Scatter plot altitude versus MPL signal strength, where all-ice (blue points) and mixed-phase (red points) clouds are distinguished using the criteria shown in the legend.

simulations, the model contains a detailed two-moment bulk treatment of stratiform cloud microphysics (26), with a detailed treatment of ice supersaturation and the vapor deposition process, as well as ice nucleation on aerosols (23). In the mixed phase, the model uses an empirical representation to nucleate ice as a function of temperature (8), as well as heterogeneous and homogenous nucleation by aerosols at temperatures <–20 °C (23). Combined with a representation of the vapor deposition (the Wegener–Bergeron–Findeisen process), the result is a rapid transition between ice and liquid at –20 °C (23), which is similar to observations in midlatitude mixed-phase clouds (27).

Simulations in this article use an updated version of cloud microphysics with prognostic precipitating hydrometeors (26, 28). Two different configurations are used. First, a single-column atmospheric model (SCAM) is used at the South Pole, with advective terms taken from a global model run forced with 2009 sea surface temperatures. Simulations are simplified by fixing the drop number and ice crystal number at 50 cm^{-3} and 5 L^{-1}, respectively. SCAM simulations prescribe initial conditions, and surface and horizontal fluxes, temperatures, and cloud species are allowed to evolve. Later, CESM is run to extend effects beyond the South Pole.

"Baseline" results of the simulations, produced by running the model without modifications, are shown in Fig. 3*A*. The frequency of occurrence of liquid water is low but would actually be much lower if it were not for the way the model implements the nucleation scheme, which nucleates and freezes water drops down to a temperature of –37 °C (8). However, there is no scheme for freezing any liquid water between –37 °C and –40 °C, the temperature in the model at which all water freezes homogeneously. This oversight in the model microphysics, which allows an artificial layer of mixed-phase cloud between –37 °C and –40 °C, is now being corrected. Even with the "artificial" supercooled liquid layer between –37 °C and –40 °C, the Baseline model run (Fig. 3*A*) predicts much less supercooled liquid water than is seen in the observations (Fig. 2*D*).

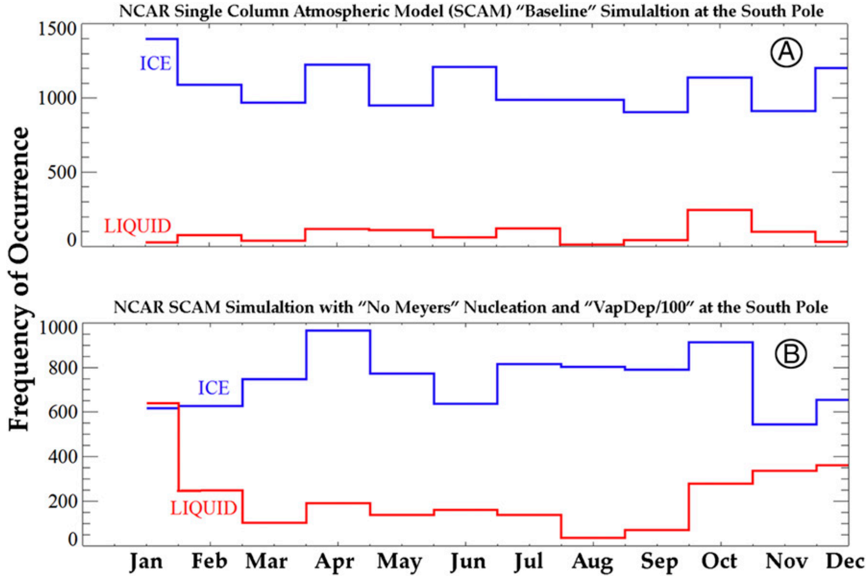

Fig. 3. (*A*) SCAM "Baseline" simulations at the South Pole occurrence of 20 min (single time step), ice (blue), and liquid (red) clouds by month. (*B*) As in *A*, except for the case where mixed-phase ice nucleation is shut off ("NoMeyers") and vapor deposition is reduced by a factor of 100 ("VapDep/100").

A detailed analysis of the microphysical process rates in the Baseline simulation indicates that the largest depletion of liquid is occurring because of an overestimate of mixed-phase ice nucleation, based on the Meyers and colleagues (1992) empirical scheme in the model (8), and because of the rapid vapor deposition of liquid onto ice. The rapid conversion is because the cloud microphysical scheme assumes perfect efficiency of the vapor deposition process, which is equivalent to assuming that the ice and liquid in clouds are well mixed to the diffusive scale. However, given turbulence and the small-scale variations of updrafts leading to variations in ice supersaturation, this assumption is probably invalid. To address these two issues, the model is altered by shutting off the mixed-phase ice nucleation scheme ("NoMeyers") and by reducing the rate of vapor deposition by a factor of 100 ("VapDep/100"), which is an arbitrary amount to nudge the simulation toward the observations. Note that these changes are intended as a sensitivity test, and a more physical treatment of these processes is warranted. The intent is to allow supercooled liquid in the model that is representative of observations at the South Pole. Ice nucleation still occurs by heterogeneous and homogeneous freezing (23). The results of rerunning the model over the South Pole with these modifications are shown in Fig. 3*B* and in Table 1. This change results in significantly more liquid and a very different annual cycle of liquid clouds (Fig. 3*B*), which agrees much better with the observations in Fig. 2*D*.

The quantitative impact of turning off the mixed-phase nucleation scheme (8) and reducing vapor deposition to provide better agreement with the observations increases the amount of liquid in clouds, which in turn affects the top-of-atmosphere (TOA) cloud radiative effect (CRE). CRE is defined as the TOA all-sky flux, minus the clear-sky flux in the absence of clouds. It can be decomposed into shortwave (SW; solar) and longwave (LW) components. Table 1 illustrates the annual averaged CRE at the South Pole (for all-sky and just cloudy-sky periods) from the Baseline case (Fig. 3*A*) and the case in which the mixed-phase ice nucleation is shut off ("NoMeyers"). Because the CRE at the South Pole is small to begin with, local radiative perturbations are modest, but as seen in Fig. 3*B*, there are considerable changes in the relative frequency of occurrence of ice and liquid clouds, with the largest effect coming in the austral summer months of December, January, and February.

The impact of increasing the ratio of supercooled liquid water in the model is to make the clouds optically thicker, which has an effect on CRE. CRE at the South Pole is small compared with at other locations because in the SW, there is very little albedo contrast with the surface, and because low clouds also mean there is little thermal contrast with the surface. In Table 1, the optically thicker clouds increase the SWCRE at TOA substantially, especially with the change in vapor deposition ("VapDep/100" and "NoMeyers + VapDep/100"). The clouds get optically thick enough to change the sign of the TOA LWCRE at the South Pole. Compared with the Baseline, the NoMeyers simulation increases the net TOA CRE when clouds are present at the South Pole from $-3.2\ Wm^{-2}$ to $-3.9\ Wm^{-2}$. The reduction of cloud frequency does mitigate the total effect somewhat. Larger effects are seen when vapor deposition is reduced (i.e., VapDep/100): The net cloudy sky effect is increased to $-5.1\ Wm^{-2}$ because the clouds get optically thicker. However, the annual average (all sky) effect is small, at $-0.26\ Wm^{-2}$ (versus $-0.8\ Wm^{-2}$ for the Baseline case).

Although the effects shown in Table 1 are important, the radiative fluxes at the South Pole represent a small region over the high Antarctic Plateau. To explore the effects of these changes beyond just the South Pole, global experiments were conducted with CESM, using fixed sea surface temperature and calendar

Table 1. SCAM simulations at the South Pole, each 1 y long with the same forcing

	SWCRE (Wm^{-2})		LWCRE (Wm^{-2})		Net CRE (Wm^{-2})	
South Pole average simulation	All sky	Cloudy	All sky	Cloudy	All sky	Cloudy
Baseline	−0.24	−1.61	−0.50	−1.62	−0.74	−3.23
NoMeyers	−0.38	−2.52	−0.42	−1.37	−0.80	−3.89
VapDep/100	−1.28	−8.41	1.02	3.32	−0.26	−5.09
NoMeyers+VapDep/100	−1.34	−8.78	1.07	3.49	−0.21	−5.39

Simulations are as indicated in the text. Shown are the top of atmosphere SWCRE, the LWCRE, and the net CRE (SW+LW) CRE. All fluxes are in Wm^{-2} and are shown for all sky, and just when clouds are present (cloudy).

Table 2. As in Table 1, except simulations are for the entire Antarctic Continent

	SWCRE (Wm^{-2})		LWCRE (Wm^{-2})		Net CRE (Wm^{-2})	
Antarctic-wide simulation	Annual	DJF	Annual	DJF	Annual	DJF
Baseline	−24.1	−33.4	18.1	11.3	−6.0	−22.1
NoMeyers	−25.1	−36.2	18.8	12.9	−6.3	−23.3
VapDep/100	−18.4	−51.4	18.8	23.6	0.4	−27.8
NoMeyers+VapDep/100	−19.0	−52.9	20.4	26.5	1.4	−26.4

Annual, effects averaged over an entire year; DJF, effects averaged over austral summer months of December, January, and February.

year 2000 boundary conditions for greenhouse gases. Table 2 indicates the Antarctic-wide average of TOA LWCRE and SWCRE, both annually and during the austral summer months of December, January, and February. As in Table 1, the simulations in Table 2 include the Baseline case, NoMeyers mixed-phase ice nucleation, reduction of the vapor deposition rate by a factor of 100 (VapDep/100), and a combination of NoMeyers + VapDep/100. Changes in TOA cloud effects in Table 2 are significant when averaged over the whole Antarctic continent: Altering the mixed-phase clouds in the simulations to produce more supercooled water, as seen over the South Pole, results in a change in SW cloud forcing in summer of $-19.5\ Wm^{-2}$ (−33.4 to −52.9, NoMeyers + VapDep/100).

This increased cooling is partially compensated by the LW (warming) changes of $+15.2\ Wm^{-2}$ ($26.5 - 11.3\ Wm^{-2}$). The change in net CRE in summer is from $-22.1\ Wm^{-2}$ in the base case to $-27.8\ Wm^{-2}$ (VapDep/100) or $-26.4\ Wm^{-2}$ (NoMeyers + VapDep/100), with a big difference in the absolute magnitude because of the optically thicker liquid clouds, which are more reflective. The effects are highly significant. During the annual cycle, the effects are different. The net CRE in the Baseline is a net cooling of $-6\ Wm^{-2}$ that shifts to a positive effect of $+1.4\ Wm^{-2}$ with the optically thicker NoMeyers + VapDep/100 case. SW cooling drops while LW heating increases, for a net warming over the continent of $+7.4\ Wm^{-2}$. Fig. 4 indicates this change is mostly over Eastern Antarctica.

The simulated radiative effects seen over Antarctica are even more significant beyond the Antarctic continent. Fig. 4 illustrates the difference in CRE when the results of the Baseline simulation are subtracted from the NoMeyers + VapDep/100 simulation and extended out over the Southern Ocean. Effects are large over the Southern Ocean storm tracks, where in situ observations show there are significant regions of supercooled liquid (29, 30). This is a different regime from the Antarctic because of the warmer temperatures (−20 °C to −30 for shallow cloud tops) and the different aerosol populations [sea salt and biogenic aerosols (31)]. However, the sensitivity test results in a doubling of the liquid water path ($40 - 90\ g^{-2}$) and a two-thirds reduction in ice water path ($18 - 6\ g^{-2}$). Cloud fractions at 60° S are similar, but increase with the sensitivity test at higher latitudes. The increase of liquid leads to large increases in the magnitude of the CRE (increased negative effects). This increase helps correct a longstanding bias in CESM for weak CREs (32) at latitudes poleward of 60° S. In this region, the cloud radiative effects are closer to observations from the energy balance adjusted flux product of the clouds and the Earth's Radiant Energy System satellite (33) in the NoMeyers + VapDep/100 than in the Baseline case. However, the global mean CREs are too large with this simple fix (designed for a different regime over Antarctica), indicating that the mixed phase is quite important for cloud forcing, but that a more complete treatment than this simple sensitivity test for regimes warmer than −30 °C is warranted.

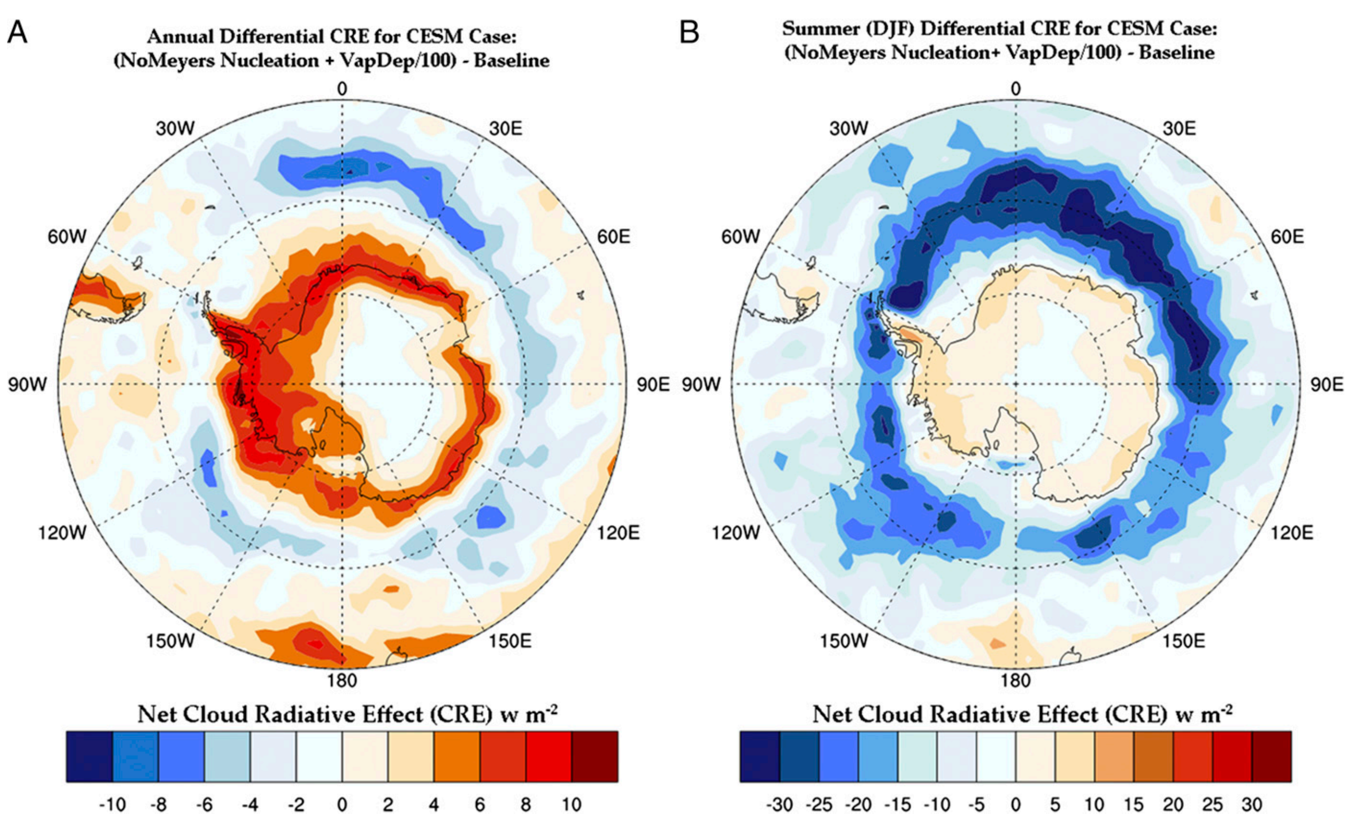

Fig. 4. (*A*) Annual and (*B*) December, January, and February differences in CRE when the CESM model results of the "Baseline" case are subtracted from the "No Meyers + VapDep/100" case.

Discussion and Conclusion

Tethered balloon in situ observations of near-surface clouds at the South Pole, coupled with closely located lidar backscatter measurements, have shown that mixed-phase clouds (supercooled liquid water coexisting with ice crystals) are more prevalent than is currently represented in global models. Mixed-phase clouds were observed in situ during the austral summer in shallow layers between about −28 °C and −32 °C. Simultaneous multipulse lidar backscatter measurements showed that water drops in mixed-phase clouds provided a strong backscatter signature not observed from all-ice clouds. Extrapolation of the lidar data to calendar year 2009 showed that water drops were present in near-surface cloud layers during 11 of 12 mo, even above strong temperature inversions, when surface temperatures were as cold as −54 °C. To estimate the impact of the new observations of mixed-phase clouds over the South Pole, sensitivity experiments were performed with constrained versions of the atmospheric component of the NCAR CESM.

Perturbations to the model cloud processes to allow supercooled liquid, as observed over the South Pole, were explored. These simple changes to mixed-phase ice nucleation and to the vapor deposition process were designed to maintain more supercooled liquid clouds in the absence of a full implementation of a more comprehensive mixed-phase cloud scheme (34). The modifications to the single-column model had the desired effect at the South Pole and are able to better represent the annual cycle and frequency of liquid clouds. Once the model microphysics were modified in a sensitivity test to maintain more supercooled liquid, significant radiative effects were seen in the South Pole simulations. The result changes the annual net CRE over Antarctica by $+7.4\ \mathrm{Wm^{-2}}$, mostly over Eastern Antarctica, which is enough to change the sign of CRE from cooling to warming. In global simulations, adjustments to the cloud microphysics change liquid and ice partitioning (and CREs) over the Southern Hemisphere storm tracks (in a warmer temperature regime) and confirm results with other models (35) that CREs are very sensitive to the representation of mixed-phase clouds and supercooled liquid. These simple sensitivity experiments will need to be replaced with improved mixed-phase and supercooled liquid parameterizations spanning temperature regimes from the South Pole to the Southern Oceans to better represent this regime in climate models.

ACKNOWLEDGMENTS. We thank Dr. Qixu Mo for his contribution to the analysis of data collected at the South Pole. The observational component of this research is sponsored under Grant OPP-0337876 from the US National Science Foundation and Grant DE-SC0006269 from the US Department of Energy. The modeling component of this research is supported by the US Department of Energy Atmospheric System Research Program Grant DE-SC0006702. The National Center for Atmospheric Research is supported by the US National Science Foundation. Micro Pulse Lidar Network (MPLNET) is funded by the NASA Earth Observing System and Radiation Sciences Program, and the South Pole MPLNET site is maintained with support from the National Oceanic and Atmospheric Administration and the US National Science Foundation Office of Polar Programs. A portion of the balloon instrument package was funded through NASA Contract NNG05CA06C.

1. Solomon S, ed (2007) *Climate Change 2007-The Physical Science Basis: Working Group I Contribution to the Fourth Assessment Report of the IPCC* (Cambridge Univ Press, New York), Vol 4.
2. Stocker TF, et al. (2013) Climate change 2013: The physical science basis. *Intergovernmental Panel on Climate Change, Working Group I Contribution to the IPCC Fifth Assessment Report (AR5)* (Cambridge Univ Press, New York).
3. Bromwich DH, et al. (2012) Tropospheric clouds in Antarctica. *Rev Geophys* 50: RG1004, 10.1029/2011RG000363.
4. Lubin D, et al. (1998) The impact of Antarctic cloud radiative properties on a GCM climate simulation. *J Clim* 11:447–462.
5. Gordon CT, Rosati A, Gudgel R (2000) Tropical sensitivity of a coupled model to specified ISCCP low clouds. *J Clim* 13:2239–2260.
6. Lachlan-Cope T (2010) Antarctic clouds. *Polar Res* 29:150–158.
7. Morley BM, Uthe EE, Viezee W (1989) Airborne lidar observations of clouds in the Antarctic troposphere. *Geophys Res Lett* 16:491–494.
8. Meyers MP, DeMott PJ, Cotton WR (1992) New primary ice-nucleation parameterizations in an explicit cloud model. *J. Applied Met.* 31:708–721.
9. Dufresne J-L, Bony S (2008) An assessment of the primary sources of spread of global warming estimates from coupled atmosphere-ocean models. *J Clim* 21:5135–5144.
10. Trenberth KE, Fasullo JT (2010) Simulation of present-day and twenty-first-century energy budgets of the southern oceans. *J Clim* 23:440–454.
11. Lawson RP, et al. (2011) Deployment of a Tethered Balloon System for Cloud Microphysics and Radiative Measurements at Ny-Ålesund and South Pole. *J Atmos Ocean Technol* 28:656–670.
12. Spinhirne JD, Rall R, Scott VS (1995) Compact eye-safe lidar systems. *Rev. Laser Eng.* 23:112–118.
13. Hurrell JW, et al. (2013) The community earth system model: A framework for collaborative research. *Bull Am Meteorol Soc* 94:1339–1360.
14. Vömel H, David DE, Smith K (2007) Accuracy of tropospheric and stratospheric water vapor measurements by the cryogenic frost point hygrometer: Instrumental details and observations. *J Geophys Res* 112:D08305, 10.1029/2006JD007224.
15. Ardon-Dryer K, Levin Z, Lawson RP (2011) Characteristics of immersion freezing nuclei at the South Pole station in Antarctica. *Atmos Chem Phys* 11:4015–4024.
16. Hu Y, et al. (2007) The depolarization - attenuated backscatter relation: CALIPSO lidar measurements vs. theory. *Opt Express* 15(9):5327–5332.
17. Zhou C, Yang P, Dessler AE, Hu Y, Baum BA (2012) Study of Horizontally Oriented Ice Crystals with CALIPSO Observations and Comparison with Monte Carlo Radiative Transfer Simulations. *J Appl Meteorol Climatol* 51:1426–1439.
18. Lawson RP, et al. (2006) Microphysical and optical properties of ice crystals at South Pole Station. *J Appl Meteorol* 45:1505–1524.
19. Heymsfield AJ, Miloshevich LM (1993) Homogeneous ice nucleation and supercooled liquid water in orographic wave clouds. *J Atmos Sci* 50:2335–2353.
20. Lawson RP, Baker BA, Schmitt CG, Jensen TL (2001) An overview of microphysical properties of Arctic clouds observed in May and July during FIRE.ACE. *J Geophys Res* 106:14,989–15,014.
21. Baker BA, Lawson RP (2006) In situ observations of the microphysical properties of wave, cirrus and anvil clouds. Part 1: Wave clouds. *J Atmos Sci* 63:3160–3185.
22. Rosenfeld D, Woodley WL (2000) Deep convective clouds with sustained supercooled liquid water down to -37.5 ° C. *Nature* 405(6785):440–442.
23. Gettelman A, et al. (2010) Global simulations of ice nucleation and ice supersaturation with an improved cloud scheme in the Community Atmosphere Model. *J Geophys Res* 115:D18216.
24. Lawson RP, et al. (2010) Microphysical and radiative properties of tropical clouds investigated in TC4 and NAMMA. *J Geophys Res* 115:D00J08, 10.1029/2009JD013017.
25. Neale RB, et al. (2010) Description of the NCAR Community Atmosphere Model (CAM5.0) (National Center for Atmospheric Research, Boulder, CO), Technical Report NCAR/TN-486+STR.
26. Morrison H, Grabowski WW (2008) A novel approach for representing ice microphysics in models: Description and tests using a kinematic framework. *J Atmos Sci* 65:1528–1545.
27. Korolev AV, Isaac GA, Cober SG, Strapp JW, Hallett J (2003) Microphysical characterization of mixed-phase clouds. *Q J R Meteorol Soc* 129:39–65.
28. Gettelman A, Morrison H (2014) Advanced Two-Moment Microphysics for Global Models. Part I: Off-Line Tests and Comparison with Other Schemes. *J Clim*, 10.1175/JCLI-D-14-00102.1.
29. Chubb TH, Jensen JB, Siems ST, Manton MJ (2013) In situ observations of supercooled liquid clouds over the Southern Ocean during the HIAPER Pole-to-Pole Observation (HIPPO) campaigns. *Geophys Res Lett* 40:5280–5285.
30. Morrison AE, Siems ST, Manton MJ (2011) A three-year climatology of cloud-top phase over the Southern Ocean and North Pacific. *J Clim* 24:2405–2418.
31. Burrows SM, Hoose C, Pöschl U, Lawrence MG (2013) Ice nuclei in marine air: Biogenic particles or dust? *Atmos Chem Phys* 13:245–267.
32. Flato G, Marotzke J (2013) Climate change 2013: The physical science basis. *Intergovernmental Panel on Climate Change, Working Group I Contribution to the IPCC Fifth Assessment Report (AR5)* (Cambridge Univ Press, New York).
33. Loeb NG, et al. (2009) Towards optimal closure of the earth's top-of-atmosphere radiation budget. *J Clim* 22:748–766.
34. Hoose C, Kristjansson JE (2010) A classical-theory-based parameterization of heterogeneous ice nucleation by mineral dust, soot and biological particles in a global climate model. *J Atmos Sci* 67:2483–2503.
35. Bodas-Salcedo A, Williams KD, Field PR, Lock AP (2012) The surface downwelling solar radiation surplus over the Southern Ocean in the Met Office model: The role of midlatitude cyclone clouds. *J Clim* 25:7467–7486.